Journal of Alloys and Compounds 645 (2015) S384–S387

Contents lists available at ScienceDirect

Journal of Alloys and Compounds

journal homepage: www.elsevier.com/locate/jalcom

XPS studies of nanocrystalline La–Ni and $LaNi_{5-x}Al_x$ ($x = 0.2, 0.5, 1$) alloy thin films

J. Skoryna *, A. Marczyńska, L. Smardz

Institute of Molecular Physics, Polish Academy of Sciences, Smoluchowskiego 17 St., 60-179 Poznań, Poland

ARTICLE INFO

Article history:
Available online 23 December 2014

Keywords:
Electronic band structure
Hydrogen absorbing materials
Photoelectron spectroscopies
Thin films
Rare earth alloys and compounds

ABSTRACT

La_2Ni_3, $LaNi_2$, $LaNi_3$ and $LaNi_{5-x}Al_x$ ($x = 0.2, 0.5, 1$) alloy thin films were prepared onto oxidised Si(100) substrates in the temperature range of 285–700 K using a computer-controlled ultra high vacuum (UHV) magnetron co-sputtering. Structural studies showed that the samples deposited at 295 K are nanocrystalline with average grain size $D \sim 15$–20 nm. Thin films deposited at about 700 K are polycrystalline with $D \sim 150$–200 nm. XPS results showed that the shape and positions of the valence bands measured for the high-purity nanocrystalline alloy thin films are similar to those determined for the polycrystalline samples. The above behaviour is in contrast to recently reported XPS valence band measured for mechanically alloyed bulk nanocrystalline $LaNi_{4.2}Al_{0.8}$ alloy, mainly due to segregation effect in the surface layer.

1. Introduction

Metal hydrides have been the subject of much recent interest stimulated in part by the technological need for adequate hydrogen storage media for application such as fuel cell vehicles [1–3]. Reversible charging and discharging at moderate temperatures together with high volumetric and gravimetric densities is required for the utilisation of hydrogen as an energy carrier. The intermetallic compound $LaNi_5$ is well known for its ability to store hydrogen reversibly at pressures and temperatures of interest for applications close to ambient conditions [1]. Therefore, it serves as a reference compound to understand the physical and chemical phenomena of the hydrogenation process.

In recent years, owing to their size dependent properties, nanodimensional materials have attracted increasing interest for basic research and applications. Materials' properties of the nanoparticles change due to the size and surface induced modifications of the electronic structures [4–7]. Several semi-empirical models [8,9] have been proposed for the heat of formation and the heat of solution of metal hydrides and attempts have been made for justifying the maximum hydrogen absorption capacity of the metallic matrices. These models showed that the energy of the metal–hydrogen interaction depends both on geometric and electronic factors. In order to optimise the choice of the nanocomposites for a selected application, a better understanding of the role of each constituent alloy on the electronic properties of the material is crucial. In a recent paper [10] we showed that the valence bands of bulk nanocrystalline and nanocomposite $LaNi_5$ based materials were broadened compared to those measured for polycrystalline samples with the similar average chemical compositions. Furthermore, practically the all mechanically alloyed nanomaterials showed significantly greater discharge capacity [10]. On the other hand, in Pd clusters hydrogen solubility increases in alpha-phase, whereas the minimum beta-phase solubility is reduced, which results in the lowering of miscibility gap compared to that measured for bulk palladium [11]. In this contribution, we study experimentally the electronic properties of polycrystalline and nanocrystalline La–Ni and $LaNi_{5-x}Al_x$ ($x = 0.2, 0.5, 1$) alloy thin films using X-ray photoelectron spectroscopy (XPS).

2. Experimental details

The La–Ni–Al alloy thin films were prepared in the temperature range of 285–700 K using computer-controlled ultra high vacuum (UHV) magnetron co-sputtering. Ni (Al) and La targets were sputtered using DC and RF modes, respectively. The total thickness of the samples was about 1000 nm. The base pressure before the deposition process was lower than 5×10^{-10} mbar. As a substrate we have used Si(100) wafers with an oxidised surface to prevent a silicide formation [12]. Therefore we have applied a special heat treatment in UHV before deposition in order to obtain an epitaxial SiO_2 surface layer [12,13]. The distance between sputtering targets and substrate was about 220 mm. The thicknesses of individual Ni, Al and La sublayers were determined by X-ray fluorescence (XRF) analysis using high purity standards and small angle X-ray diffraction. Basing on above described thickness calibrations the average compositions of the thin film samples were controlled by varying deposition rates of Ni, Al, and La. Typical sputtering conditions used during La–Ni–Al alloy thin films deposition are listed in Table 1. Furthermore, the deposition rates were individually checked by quartz thickness monitors. Using the stable deposition rates for sputtered Ni, Al, and La targets we have assumed the average atomic compositions of prepared thin film alloys as: La_2Ni_3, $LaNi_2$, $LaNi_3$ and $LaNi_{5-x}Al_x$ ($x = 0.2, 0.5, 1$).

---

* Corresponding author.
E-mail address: jskoryna@ifmpan.poznan.pl (J. Skoryna).

http://dx.doi.org/10.1016/j.jallcom.2014.12.104
0925-8388/© 2014 Published by Elsevier B.V.

The surface chemical composition and the cleanness of all layers was checked immediately after deposition, transferring the samples to an UHV (4×10^{-11} mbar) analysis chamber equipped with XPS, Auger electron spectroscopy (AES) and ion gun etching system. The XPS core level and valence band spectra were measured with Al Kα radiation at 1486.6 eV at room temperature using a SPECS EA 10 PLUS energy spectrometer. The energy spectra of the electrons were analysed by a hemispherical analyser ($\mathrm{FWHM}_{\mathrm{Mg\ K}\alpha} = 0.8$ eV for Ag $3d_{5/2}$). All emission spectra were measured immediately after sample transfer in a vacuum of 8×10^{-11} mbar. Details of the XPS measurements can be found in Ref. [10].

The morphology and roughness for the representative thin film samples were studied by UHV scanning tunneling (STM) and atomic force (AFM) microscopy. The structure of the prepared alloy thin films was examined by standard θ–2θ X-ray diffraction with Cu Kα radiation.

3. Results and discussion

Results on XRF measurements revealed the assumed bulk chemical composition of the prepared alloy thin films. Structural studies showed that the samples deposited at 285 K are nanocrystalline with average grain size $D \sim 15$–20 nm. Thin films deposited at about 700 K are polycrystalline with $D \sim 150$–200 nm. Details concerning structural characterisation of the samples will be published in a separate paper [14].

In Fig. 1 we show XPS core-level spectra of the freshly deposited nanocrystalline La_2Ni_3, $LaNi_2$, and $LaNi_3$ thin films. Due to well known high reactivity of lanthanum with oxygen we have prepared the nanocrystalline alloy thin films after an additional heating of the sample holder and new substrate at 700 K for 3 h and cooling to 285 K. Results showed that after such an outgassing procedure, it is possible to prepare oxygen and carbon free La–Ni surface. The corresponding XPS spectra are shown in Fig. 1. If the outgassing procedure is too short, the sample holder before deposition will not be perfectly clean. Moreover, if the XPS measurements were performed after few hours delay the sample surface would already be partly oxidised, despite the vacuum of 4×10^{-11} mbar in our analysis chamber. In that case the intensity of the XPS signal decreases and the valence band could be artificially broadened. In our case, the oxygen and other surface impurities are practically absent on such prepared La-based alloy thin films immediately after deposition. As can be seen in Fig. 1, practically no XPS signal from potential contamination atoms like O-1s and C-1s is observed. On the other hand, we have observed oxygen atoms (below 1 at.%) already adsorbed on La_2Ni_3 surface 1 h after preparation. Note that the sample was kept in the analysis chamber in vacuum of 4×10^{-11} mbar.

We have prepared $LaNi_{5-x}Al_x$ ($x = 0.2, 0.5, 1$) thin films using very similar method including above described outgassing procedure of the substrate and holder. Fig. 2 shows XPS spectra of nano- and polycrystalline $LaNi_4Al_1$ thin films prepared at a substrate temperature of 285 K and 700 K, respectively. The oxygen, carbon and other surface impurities or adsorbates are practically absent immediately after deposition on such prepared alloy surfaces.

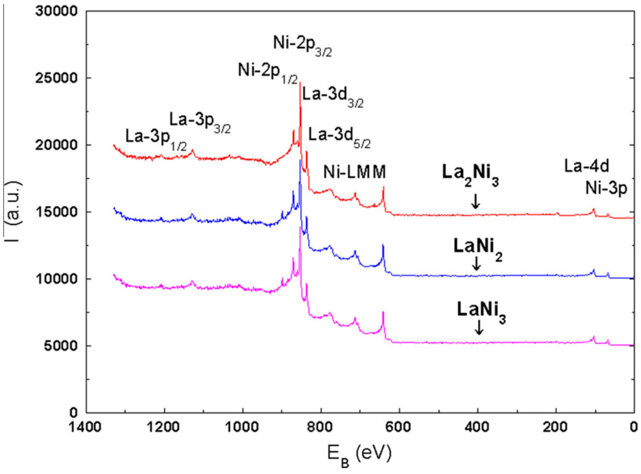

Fig. 1. XPS (Al Kα) spectra of the freshly prepared nanocrystalline La_2Ni_3, $LaNi_2$, and $LaNi_3$ thin films.

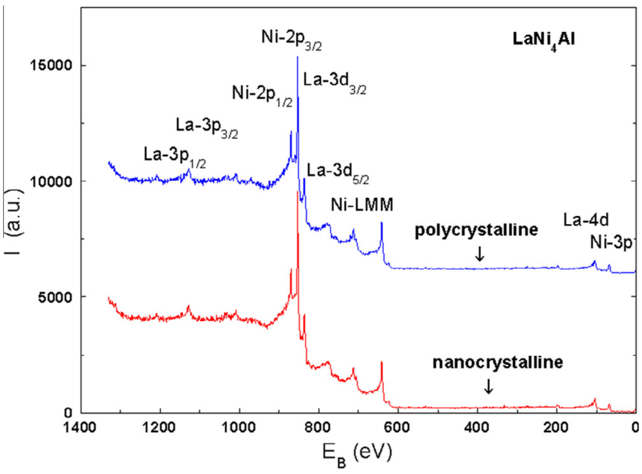

Fig. 2. XPS (Al Kα) spectra of the freshly prepared nano- and polycrystalline $LaNi_4Al$ alloy thin films.

In previous papers [15,16] we have reported a strong segregation of the La atoms to the surfaces in mechanically alloyed bulk nanocrystalline $LaNi_5$-type alloys under ambient conditions. However, the XPS studies performed immediately after deposition showed no remarkable segregation of La atoms to the surface in nanocrystalline or polycrystalline La-based alloy thin films (see Figs. 1 and 2). It was also revealed in the La-3d and Ni-2p spectra measured with higher resolution (not showed here). On the other hand, preliminary XPS studies with depth profiling show the La segregation effect after 24 h of thin film exposition to the ambient conditions (contact with atmosphere).

In Fig. 3 we show the XPS valence bands for nanocrystalline La_2Ni_3, $LaNi_2$, and $LaNi_3$ thin films. The shape of the valence band

Table 1
Typical sputtering conditions used for deposition of La–Ni–Al alloy thin films.

Parameter	Unit	La	Ni (Al)
Rest gas pressure	mbar	5×10^{-10}	5×10^{-10}
Argon partial pressure	mbar	6×10^{-4}	6×10^{-4}
Argon purity	%	99.9998	99.9998
Target diameter	mm	51.5	51.5
Target purity	%	99.99	99.999
Distance between substrate and target	mm	220	220
Sputtering method		Magnetron RF	Magnetron DC
Sputtering power	W	30–70	20–60 (20–40)
Deposition rate	nm/s	0.01–0.07	0.01–0.1 (0.01–0.6)
Substrate temperature during deposition	K	285 (nanocrystalline) 700 (polycrystalline)	285 (nanocrystalline) 700 (polycrystalline)